Gerda

Progress Report to the LNGS Scientific Committee

Version 1.0

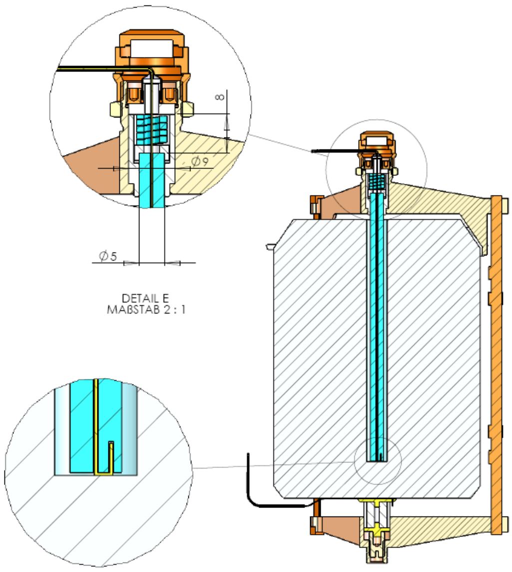

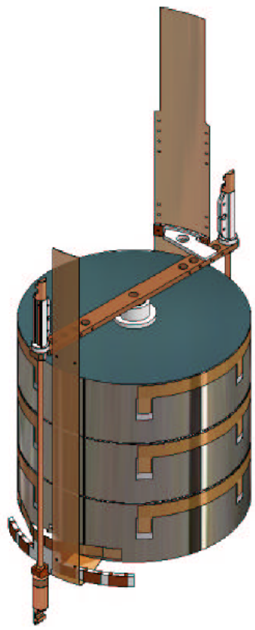

September 2005

I. Abt [j], M. Altmann [j], A.M. Bakalyarov [i], I. Barabanov [g], C. Bauer [c], M. Bauer [l], E. Bellotti [f], S. Belogurov [g,h], S.T. Belyaev [i], A. Bettini [k], L. Bezrukov [g], V. Brudanin [b], V.P. Bolotsky [h], A. Caldwell [j], C. Cattadori [a,f], M.V. Chirchenko [i], O. Chkvorets [c], E. Demidova [h], A. Di Vacri [a], J. Eberth [d], V. Egorov [b], E. Farnea [k], A. Gangapshev [g], J. Gasparro [m], P. Grabmayr [l], G.Y. Grigoriev [i], V. Gurentsov [g], K. Gusev [b], W. Hampel [c], G. Heusser [c], M. Heisel [c], W. Hofmann [c], M. Hult [m], L.V. Inzhechik [i], J. Jochum [l], M. Junker [a], S. Katulina [b], J. Kiko [c], I.V. Kirpichnikov [h], A. Klimenko [b,g], M. Knapp [l], K.T. Knöpfle [c], O. Kochetov [b], V.N. Kornoukhov [g,h], K. Kröninger [j], V. Kusminov [g], M. Laubenstein [a], V.I. Lebedev [i], X. Liu [j], B. Majorovits [j], G. Marissens [m], I. Nemchenok [b], L. Pandola [a], P. Peiffer [c], A. Pullia [f], C. Rossi Alvarez [k], V. Sandukovsky [b], S. Schönert [c], S. Scholl [l], J. Schreiner [c], U. Schwan [c], B. Schwingenheuer [c], H. Simgen [c], A. Smolnikov [b,g], F. Stelzer [j], A.V. Tikhomirov [i], C. Tomei [a], C.A. Ur [k], A.A. Vasenko [h], S. Vasiliev [b,g], D. Weißhaar [d], M. Wojcik [e], E. Yanovich [g], J. Yurkowski [b], S.V. Zhukov [i], F. Zocca [f], G. Zuzel [c]

[a] INFN Laboratori Nazionali del Gran Sasso, Assergi, Italy
[b] Joint Institute for Nuclear Research, Dubna, Russia
[c] Max-Planck-Institut für Kernphysik, Heidelberg, Germany
[d] Institut für Kernphysik, Universität Köln, Germany
[e] Jagiellonian University, Cracow, Poland
[f] Università di Milano Bicocca e INFN Milano, Milano, Italy
[g] Institute for Nuclear Research of the Russian Academy of Sciences, Moscow, Russia
[h] Institute for Theoretical and Experimental Physics, Moscow, Russia
[i] Russian Research Center Kurchatov Institute, Moscow, Russia
[j] Max-Planck-Institut für Physik, München, Germany
[k] Dipartimento di Fisica dell'Università di Padova e INFN Padova, Padova, Italy
[l] Physikalisches Institut, Universität Tübingen, Germany
[m] Institute for Reference Materials and Measurements, Geel, Belgium

Spokesperson: S. Schönert,
(Stefan.Schoenert@mpi-hd.mpg.de)
Co-Spokesperson: C. Cattadori
(Carla.Cattadori@lngs.infn.it)
Technical Coordinator: K.T. Knöpfle
(Karl-Tasso.Knoepfle@mpi-hd.mpg.de)

URL: http://www.mpi-hd.mpg.de/GERDA/

Contents

1 Executive summary

Major progress has been accomplished over the last six months. This includes the process of refurbishment of the existing enriched detectors, the design of new segmented detectors, the procurement of new enriched ^{76}Ge material, the development and testing of the analog and digital electronics, the screening and selection of ultra pure materials for detector constructions, the Monte Carlo simulations of signals and backgrounds, as well as the experimental infrastructures in hall A. The latter consists of the integrated design of the water tank, the cryogenic vessel, the super-structure and the infrastructures on top of the tank.

A series of safety review meetings with LNGS engineers and external safety experts have taken place during the last six months. Several safety analysis documents have been worked out as for example a Failure Modes Effects and Criticality Analysis (FMECA), a Hazard and Operability Study (HAZOP), a safety study of the TÜV Nord, as well as a second-opinion on the GERDA risk assessment. Following the recommendations of the LNGS safety experts, the GERDA collaboration is currently investigating the insertion of an additional wall between cryostat and water vessel in order to further minimize the risk of mixing cryogenic liquid and water. In addition, an evacuation plan is being prepared for the case of excessive LN or LAr evaporation. At present, we are investigating the specifications of such a third wall to determine if it is compatible with the physics goals of GERDA, and feasible within the available financial resources. After clarification of this issue and following the safety approval by the LNGS, we plan to proceed with the respective tendering and ordering processes of the water tank, the super-structure and the cryogenic vessel.

A detailed time schedule of the GERDA project has been worked out including the interdependencies during the construction and commissioning phases. It is planned that 16 months after start of tendering we will commence operations of enriched detectors in the cryogenic tank and start Phase I of GERDA. The time delay necessitated by the evaluation of the 'third wall' recommendation is expected to be a few months. The new detectors for Phase II are presently expected to be ready in 2007. If this date is realized, the time lag between Phase I and Phase II will be considerably reduced.

With the approval of financial requests to the Italian INFN and the German BMBF, the funding situation of GERDA has further improved. Moreover, the collaboration could strengthen its expertise in low-background measurements through the participation of Mikael Hult and his group from the Institute for Reference Materials and Measurements, Geel, Belgium. The group and their HADES underground laboratory nearby Olen provides important support for screening measurements, as well as for underground storage during detector production and refurbishment.

2 Refurbishment of enriched detectors for Phase I

The refurbishment and testing of the former HdM and Igex detectors for their use in Phase I of Gerda is broken into a number of work packages as described in the last report. WP1 concerns the installation of a new underground detector laboratory (ie. the LArGe–Facility), WP2 deals with the testing of the HdM and Igex detectors prior to refurbishment, WP3 comprises the design, construction and testing of new low-mass detector optimized for the existing crystals, and WP4 regards the the mounting and testing of the enriched diodes into the new support system. The progress of the different work packages is summarized below.

2.1 Underground detector laboratory (LArGe–Facility)

The refurbishment of the barrack is completed including the modification of the air ventilation and hepa-filter system. It is now transformed to a clean room and equipped as an underground detector laboratory.

The new laboratory installations include a fume hood with a charcoal filter, a clean bench, and a wash stand with de-ionized water supply. Moreover, a new detector test stand is ready for transportation to Gran Sasso. It consists of a hermetically closed clean bench which can flushed with gaseous nitrogen to avoid radon contaminations. It is connected to a liquid nitrogen dewar system which will be used for testing the spectroscopic performance of the refurbished detectors.

The main parts of the LArGe shielding system to test the liquid argon scintillation read out concept has been mounted. The copper dewar, photomultiplier as well as the radon lock and suspension system are under preparation.

The underground detector laboratory will become fully operational during the upcoming months.

2.2 Characterization of the existing enriched germanium diodes

Characterization and testing of the former HdM detectors with radioactive sources have been completed. As reported, the energy resolution of all crystals is the same, or in some cases even better compared to the resolution published by the HdM experiment. One cryostat shows a degraded vacuum and it is planned to perform a 'heat and pumping cycle'. Further characterization measurements with radioactive sources will be carried out until the detectors will be dismounted and the crystals refurbished.

For logistics reasons, the Igex detectors are still stored underground at the Canfranc laboratory. The date of transportation is under discussion with the Russian, Spanish and US partners involved. We are confident to move them to Gran Sasso before the end of this year. Test measurements of the detectors in their cryostat using gamma sources will be carried out subsequently at Gran Sasso.

2.3 Low-mass detector support and contacts

The design of the new detector support and contacts has been completed and a first prototype built. Figure 1 shows some details of the design and a photo of the prototype detector. The design is optimized to fit the existing HdM and Igex crystals and their particular contact scheme. The inner contact pin as well as the spring to apply forces onto the pin are made out of single-crystal silicon. Other materials used are NOSV copper from the Nordeutsche Affinerie and PTFE.

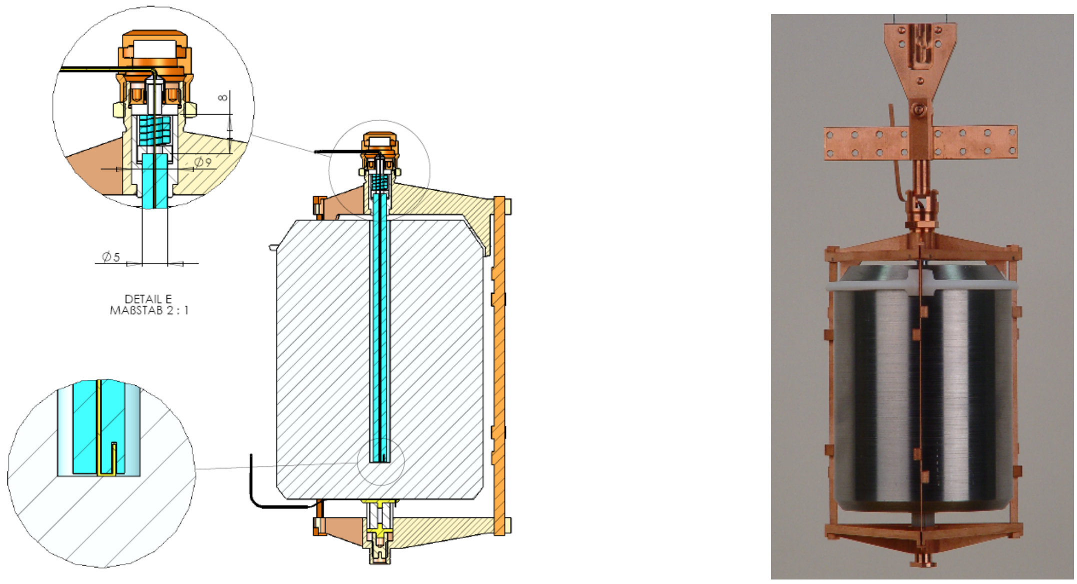

Figure 1: Left: Drawing of detector support and electrical contacts for Phase I detectors. The signal contact is pressed to the bottom by a pin and spring, both made out of silicon. Right: mechanical prototype of a Phase I detector.

First mechanical and thermal tests with the prototype detector have been completed successfully. The mechanical prototype was submerged in liquid nitrogen and all mechanical parts inspected both at liquid nitrogen and room temperature. Next steps include the testing of the electrical contacts using (non-enriched) germanium crystals, as well as a full operational test of a detector assembly.

In Monte Carlo studies using the MaGe Geant4 framework, we investigated the background induced by the detector support and contacts. As input numbers we used the upper limits obtained from screening measurements with the GeMPI detector for copper and PTFE, and from NAA measurements of silicon. The calculated maximal background due to the detector holder and electrical contacts is $< 1.5 \cdot 10^{-3}$ cts/(keV·kg·y) with similar contributions from copper and from PTFE. The design thus meets the specifications of Phase I, ie. $< 1 \cdot 10^{-2}$ cts/(keV·kg·y). The materials for the low-background detector support have been procured and undergo final screening with the GeMPI detector at Gran Sasso.

Close cooperation has been established with an European detector company. A detailed plan has been worked out in case that the refurbishment of the enriched detectors would require operations which can not be carried out underground. This includes for example a new boron implantation, or the evaporation of a new passivation layer.

Mounting and contacting the enriched diodes in new support structure, as well as the characterization of detector performance with respect to signal response and radioactive background (WP4) will start after successful completion of the prototype testing of WP3.

3 New detectors for Phase II

The production of new detectors for Phase II is under preparation. About 20 kg of HP-Ge crystals, enriched in ^{76}Ge, will be fabricated. The project is broken into work packages concerned with germanium enrichment, crystal production, as well as developing and testing of segmented detectors.

3.1 Germanium Procurement

Enrichment: Germanium enrichment is done by ultracentrifugation of gaseous GeF_4 at the company ECP in Zelenogorsk, Russian Federation. A purchase order to produce 37.5 kg of Germanium, enriched to a level of at least 86% in ^{76}Ge, has been placed. Enrichment of this sample was started in February 2005 and has been completed by beginning of September 2005. Enrichment is done in GeF_4, which afterwards is converted to GeO_2. At several steps in the production chain samples for quality control were taken. Various analytical techniques are employed for quality control measurements, among them spark source and glow discharge mass spectrometry (SSMS, GDMS), ICP-MS, and ICP-EAS.

Optimization of the Enrichment Process: The Gerda collaboration and ECP have co-operated in tuning the employed equipment and re-engineering the handling procedures, in order to maintain the purity of the starting material as much as possible during the entire process. It has been possible to reach a purity of the enriched material of up to 99.99 %, substantially better than the 99.8 % which were originally achieved. In addition, by optimizing the batch size the average time where the material remains above ground while enrichment is proceeding could be reduced. The produced batches are stored underground at the ECP site until the entire quantity is enriched. The average time above ground after centrifugation is only 3.1 d, and the storage time underground (ca. 10 mwe) is an average of 120 d.

Chemical Purification: Preceding crystal growing, chemical purification of the GeO_2 is usually done, before the oxide is reduced to produce 'semiconductor grade' metallic Germanium. Tests were performed to see if the higher quality of the enriched material would allow to skip this step, with negative results. Typically, this purification has a yield of only ≈ 70 %. R&D on chemical purification has led to the development of an improved technique with an expected overall yield of more than 85%.

Transport: The enriched material is transported from Siberia to the interim underground storage site by road transport. Transport time from Zelenogorsk to Western Europe is about 3 weeks, depending on road conditions and delay times experienced at border crossings. During transport, the material is stored inside a specially designed protective steel container (PSC). The PSC reduces activation of the Germanium by the hadronic component of cosmic rays by about a factor of 10-15. In order to discover possible unforeseen problems and time-delays a 'test transport' with 15 kg of natural (i.e. non-enriched) Germanium, was done. Like the 37.5 kg of ^{76}Ge, the 15 kg sample of natural Germanium, chemically purified to 99.9999%, was produced in Siberia. It was shipped in exactly the same way as foreseen for the enriched sample. In addition to testing the logistics, the natural Germanium sample serves to tune the techniques and instruments employed for material quality checks and as a test batch for crystal production and detector fabrication. Procurement of the natural germanium has been successfully concluded; the natural sample was received at MPI Munich on March 7, 2005 after a 20 day transport time. After unloading of the Germanium, the PSC was sent back to ECP in order to be re-used for the transport of the enriched material.

3.2 Crystal Production

The first stages of crystal production are further purification of the Germanium via polyzone and consecutive monozone refinement. These are followed by the actual crystal pulling step, employing the Czrochalski technique, by characterization of the crystal properties, and finally by mechanical cutting and shaping of the raw crystal to the specified dimensions. Discussions with crystal growing companies are ongoing, with the aim of adapting their equipment and procedure towards achieving a high yield for our sample (which is a small quantity compared to the batch sizes they usually operate with).

3.3 Segmented Germanium Detectors

Detector Development and Characterization: For Phase II of the experiment a customized detector design is used. The Germanium crystals will be of "true coaxial" type and have a segmented outer electrode. Detailed Monte Carlo simulations based on Geant 4 have been performed to study the performance of segmented detectors. Segmentation will be 6-fold in ϕ and 3-fold in z, i.e. along the core axis. Segmentation and, in addition, pulse-shape analysis can be used as powerful, complementary tools to reveal the microscopic topology of charge deposition in the crystal, serving to substantially reduce background levels. Background reduction of about one order of magnitude seems feasible by exploiting a combination of both methods. Segmented prototype detectors for both n- and p-type crystals are available. They are not yet low-background and are used for laboratory tests, in order to gain operational and handling experience and to develop readout and analysis tools. Test facilities suitable for both detector options are under construction and a variety of measurements characterizing the detectors are being prepared. Special emphasis is put on (i) the measurement of pulse-shapes in all detector regions, (ii) the influence of impurities and orientation of the crystal axis on pulse-shapes, and (iii) the characterization of dead detector layers. These measurements will be conducted both in vacuum and in liquid nitrogen.

Detector Suspension: In the GERDA experiment the detectors are mounted in a modular, scalable arrangement of strings. Each string can hold a maximum of up to 5 detectors. Strings are arranged in a hexagonal structure. The strings are composed of detector units which are individually produced. They are connected to form a string just before loading into the cryostat. A detector unit as depicted in fig. 2 consists of the following components: Germanium crystal, suspension system, HV cable, and segment signal cable.

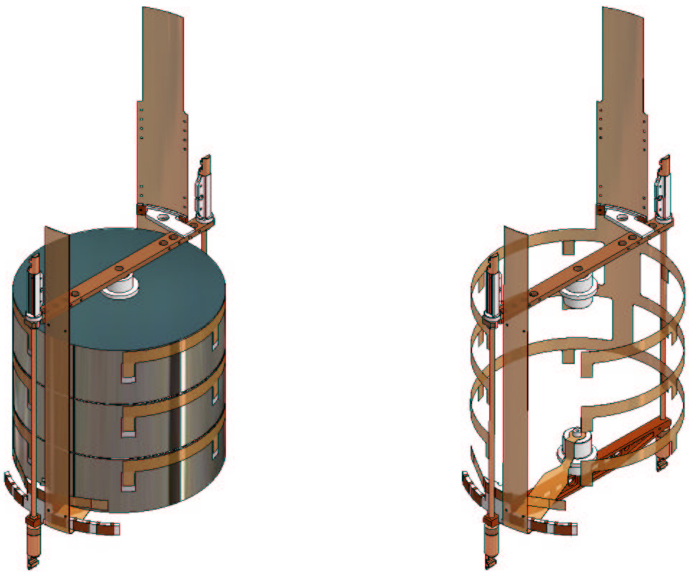

Figure 2: Left: Detector unit including crystal, suspension and cables. Right: Detector unit without crystal. The segment-signal cable is on the back, the HV-cable is on the front side. Both cables are attached to Teflon pieces which are integrated into the copper suspension.

The suspension system is constructed entirely out of copper and Teflon. The copper parts provide the main support through a clamp system with two vertical rods, a main holder at the bottom and a stabilizing bar at the top. The detector crystal rests between Teflon pieces. Special Teflon pieces attached to the copper bars allow the fixation of the cables. Samples of all materials are being screened for radioactivity. The Kapton itself and the components of the Kapton cables are under investigation. Limits on the allowable contamination come from Monte Carlo studies. These studies were done using the MaGe framework.

4 Diode readout and signal processing

In the last semester, the activity on the front-end devices has focused on the characterization of three existing solutions and on the development of ASIC CMOS circuits, custom designed for GERDA.

AGATA hybrid preamplifier[1]+BF862 FET: This preamp with excellent performance has been developed in the framework of AGATA. It is a hybrid with BJT devices and, therefore, cannot be operated at cryogenic temperatures. The BF862 JFET would be located in the junction box close to the diode at cryogenic temperatures and the preamp outside at room temperature. Therefore, for each channel the JFET and its preamp will be connected by two 6 meter coaxial cables to close the feedback loop.

Table 1 shows both the native performances of the AGATA preamp when the JFET-preamp distance is 10-20 cm, and the obtained performances in the GERDA configuration when they are 6 m apart. In the latter case, it is necessary either to increase the internal capacitance of the amplifying node of the preamplifier and, consequently, to reduce the bandwidth to eliminate the large ringing of the pulse induced by the propagation delay of 6 m cable, or to accept the pulse ringing and then to deconvolute the signal using numerical filtering techniques called “deoscillation filter” (Fig. 3). In both cases, the rise time and equivalent noise charge (ENC) figures are within the GERDA specifications. The deoscillation filter leads to better results for the rise time (33 ns vs 80 ns). For GERDA, it is very significant that the deoscillation method allows also to reconstruct structures in the rising edge of the input pulse, as shown in Fig. 4. Instead, if the preamplifier bandwidth is reduced by using a compensation capacitance, the step in the signal structure is much less evident. Therefore the numerical deoscillation filter allows a better pulse shape analysis.

IPA4[2]: The I(ntegrated)PreA(mplifiers)(v)4 is a monolithic JFET design built in the buried layer technique. It has been developed in the ’90s for LAr and LKr calorimetry for detectors with large input capacitances and is produced by InterFET. Given its excellent noise figure, a version for $C_D \approx 10$ pF has been designed.

Since this device is a monolithic JFET circuit, it can work at cryogenic temperatures, even if the LN temperature is not the optimal one in terms of noise due to the charge carrier freeze-out phenomenon. We have tested the IPA4 both at room and at cryogenic temperatures. The obtained rise time and noise figures are listed in table 1 as well. This device is appealing for GERDA, since it is integrated and it can be operated in the junction box at an increased temperature due to its self-heating. However the IPA4 doesn’t drive

	T [K]	Sensitivity [mV/MeV]	rise time [ns]	ENC/shaping time [num. of e^-]/[μs]	power [mW]
AGATA+BF862^A (short cable)	300	150	6.5	145/2	220
AGATA+BF682^B (long cable)	300 77	150	80	156/2 180/10	220
AGATA+BF682^C (deoscillation filter)	77	150	33		220
IPA4^D IPA4^E	300 300 77 ≈120	150 75 75 75	400 120-160 40	110/10 110/10 135/10	50
AMPTEK 250^E + SK152	300 77	55 55	27 37	150/2 190/2	

Table 1: Measured characteristics of the three preamplifiers options in the GERDA configuration. The capacitance of the cable between the detector and the input JFET is not known yet and is not taken into account in the noise figures.

^{A} Detector capacitance $C_D = 27$ pF, feedback capacitance $C_f = 1.5$ pF

^{B} $C_D = 23$ pF, $C_f = 1.0$ pF, 6 m cable between JFET-preamp, $C_{comp} = 33$ pF

^{C} $C_D = 23$ pF, $C_f = 1.0$ pF, 6 m cable between JFET-preamp, no C_{comp}

^{D} $C_D = 23$ pF, $C_f = 0.5$ pF

^{E} $C_D = 23$ pF, $C_f = 1.0$ pF

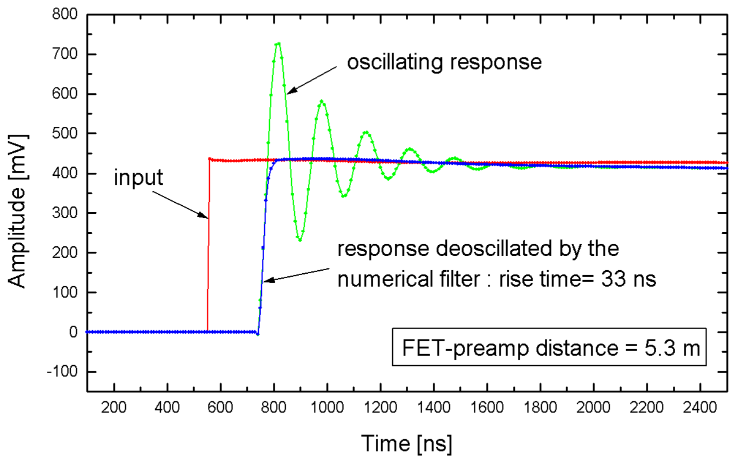

Figure 3: The preamplifier response is deconvoluted through a numerical FIR filter ("deoscillation filter"). The obtained rise time is 33 ns.

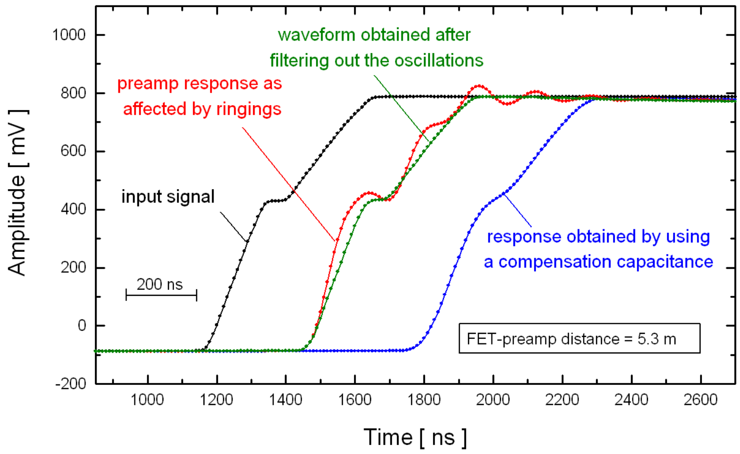

Figure 4: A pulse with a structure in its rising edge is fed into the uncompensated preamplifier (affected by ringing). The signal shape becomes hardly recognizable. However it is nicely reconstructed after passing the signal through the deoscillation filter. As a comparison, the signal obtained with a compensation capacitor in the preamplifier is shown.

50 Ω load and the rise time is quite large unless the feedback capacitance in increased and hence the sensitivity is decreased. For temperatures of about 120 K the rise time reaches 40 ns which is quite acceptable. For a shaping time of 10 μs the noise is 110 e^- r.m.s. and 135 e^- r.m.s. at 300 K and 77 K, respectively.

AMPTEK 250 + SK152[3]**:** We have also investigated the AMPTEK 250 commercial hybrid preamplifier. It is developed for the MARS PathFinder mission to read out the α-, X-, and gamma spectrometer. Its characteristics are listed in table 1. This circuit is very small (0.8" x 0.5"), has low power consumption, and is mounted in a 14-pin socket closed in a metal package. It can be coupled to many FETs to match C_D and the proper application. Even if its specifications do not include cryogenic operation, we found that it is still working once immersed in LN with only moderate degradation of performance.

CMOS ASIC circuits: We already started to work on an ASIC circuit built in CMOS technology, given the improvements in terms of noise obtained with this technique. While for GERDA Phase I, thanks to the limited amount of channels one of the above listed solution is viable, for Phase II an integrated readout device will be mandatory, as the number of readout channels will increase by a factor of 20-30. A circuit having the proper characteristics to match gamma spectrometry specifications in terms of noise, gain, stability, etc. has been designed by A.Pullia (Milano INFN and University) and submitted for production in AMS 0.8 μm technology to EUROPRACTICE. The first preamps together with test structures and single components will be delivered in the middle of October 2005. Another CMOS ASIC circuit is currently under development in Heidelberg. The ASIC lab in Heidelberg has some experience with charge sensitive preamplifiers and the collaboration decided to follow a parallel approach for an integrated chip design. The first chip is expected to be delivered in February 2006.

5 DAQ Electronics and software

Several options for the FADC system of GERDA have been evaluated over the last months. Most promising solutions are the MD^{2}S system developped by the Padova group of GERDA in the framework of the AGATA project and the commercial VME card SIS3301 of Struck. Even if the performance tests are not fully finalized, both solutions are found to be adequate in terms of analog performance. The SIS3301 is more compact and can also be used for the second phase of the experiment. The MD^{2}S option is completely developped and offers a cost advantage. Provided financial support of INFN it can be built in a short time. In addition, the readout and analysis software for the MD^{2}S system exists already. Adoptions for the SIS3301 card are foreseen.

The tests also showed that for a long term stability of the system the DAQ has to be housed in a temperature controlled environment.

Currently, the final decision on the FADC for phases I and II of GERDA is still pending. The specification of the slow control for monitoring of the experiment will start once more information about the total infrastructure is available. The Padova group has taken over the major responsibility for the DAQ.

6 Cryogenic vessel

The cryostat contains the liquid nitrogen (LN) or argon (LAr) in which the Ge diodes are operated. The cryogenic liquid serves simultaneously as a shield against the remnants of the external γ background penetrating the surrounding water shield and the cryostat's own radioactivity. The baseline is a super-insulated cryostat manufactured predominantly from radiopure ($<19\mu$Bq/kg ^{228}Th) copper; the fall-back solution is a super-insulated stainless steel cryostat with an internal lead or copper shield in the cold volume. Basic specifications include an earthquake tolerance of 0.6 g and a daily evaporation rate of <0.2 %.

Figure 5 shows the almost final layout of the super-insulated copper cryostat. The inner container (KIG) rests on six plastic pads (see detail at lower left); a stainless steel bellow in the neck connects the inner with the outer (KAG) container. Two further sets of radially pointing plastic pads at top and bottom are used to center inner and outer container (details in right part). The alternative design where the inner container is suspended at the neck has been abandonned in order to minimize the stress in the neck. Further improvements as compared to the previous version have been worked out in contacts with the TÜV Nord as well with the manufacturing parties. They include (i) the use of high-purity OFE copper insted of DHP copper as construction material which will yield higher radiopurity and better electron beam welding properties, (ii) the exchange of hemispherical heads which would have been welded from eight segments by Korbbogen heads which can be pressed as one piece from a single copper metal sheet, and (iii) the compliance of the design with the framework 'Basissicherheit von druckführenden Komponenten' (BSK - base safety for pressurised components) which is used for the design and construction of German pressurised-water reactors.

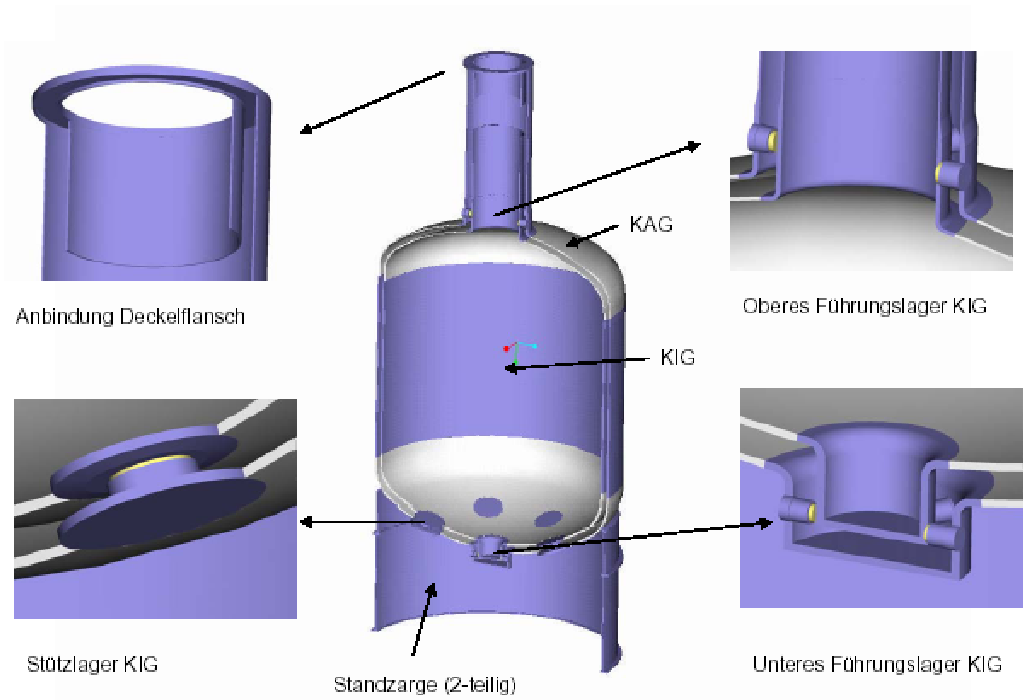

Figure 5: General layout and some details of the super-insulated copper cryostat.

The safety review of the cryostat and water vessel system has been started in spring by the submission of a first version of the Technical Proposal to LNGS. Based on this proposal a Failure Modes Effects and Criticality Analysis (FMECA) and Hazard and Operability Study (HAZOP) has been worked out by Air Liquide and presented in a final meeting at LNGS on July 5. Both analyses show the GERDA cryostat system to be safe if constructed 'correctly'. On the other hand, the unusual configuration of the cryostat immersed in a water bath of practically unlimited heating power has made the LNGS safety experts to express concerns, in particular, (i) if the proposed cryostat is indeed a double-wall container, and (ii) if the probability for rupture of one shell is low enough for underground use. In response to the latter concern, a document of the TÜV Nord has been prepared that states the probability for leakage of a single cryostat wall to be $<10^{-7}$ per year if designed and fabricated according to the BSK and concludes that the risk for the underground laboratory resulting from the cryostat operation can be disregarded.

A second-opinion on the GERDA risk assessment ordered by LNGS does, however, not accept the conclusions of the TÜV Nord report. It quotes the policy of the Health and Safety Executive according to which low frequency events (10^{-6} to 10^{-8} per year) with potential catastrophic consequences should be 'tolerated' only if the risk has been reduced 'as low as reasonably practicable' (ALARP). In this spirit, the second-opinion report recommends the insertion of an additional wall between cryostat and water vessel in order to further minimize the risk of mixing cryoliquid and water as well as the preparation of an evacuation plan for the case of excessive LN or LAr evaporation. Sharing the goal at arriving at an optimal safety concept, the GERDA collaboration has acknowledged the second-opinion report, and it is investigating at present if such a third wall is compatible with the envisaged physics performance of GERDA and feasible within its financial capabilities.

The fabrication of the copper cryostat is presently prepared by the certification of the electron beam welding procedures for copper-copper and copper-stainless steel welds. For this purpose, 1 ton of OFE copper has been ordered at the Norddeutsche Affinerie in order to be rolled according to the TÜV's specifications. Using this material, also the pressing of the Korbbogen head will be tested. By this procedure, the full production cycle will be tested and certified already before the actual vessel fabrication.

With the safety approval by the LNGS, also the process of ordering the cryogenic infrastructure can be continued. All the parties which expressed their interest to tender upon our *'Prior Information Notice'* - SIMAP-MPI-K 31 Jan'05 ID:2005-002331 will be informed about the opening of the tendering process. The rather detailed 'Piping and Instrumentation Diagram' (PID) prepared within the HAZOP analysis (Fig. 6) will provide the basis for this tender.

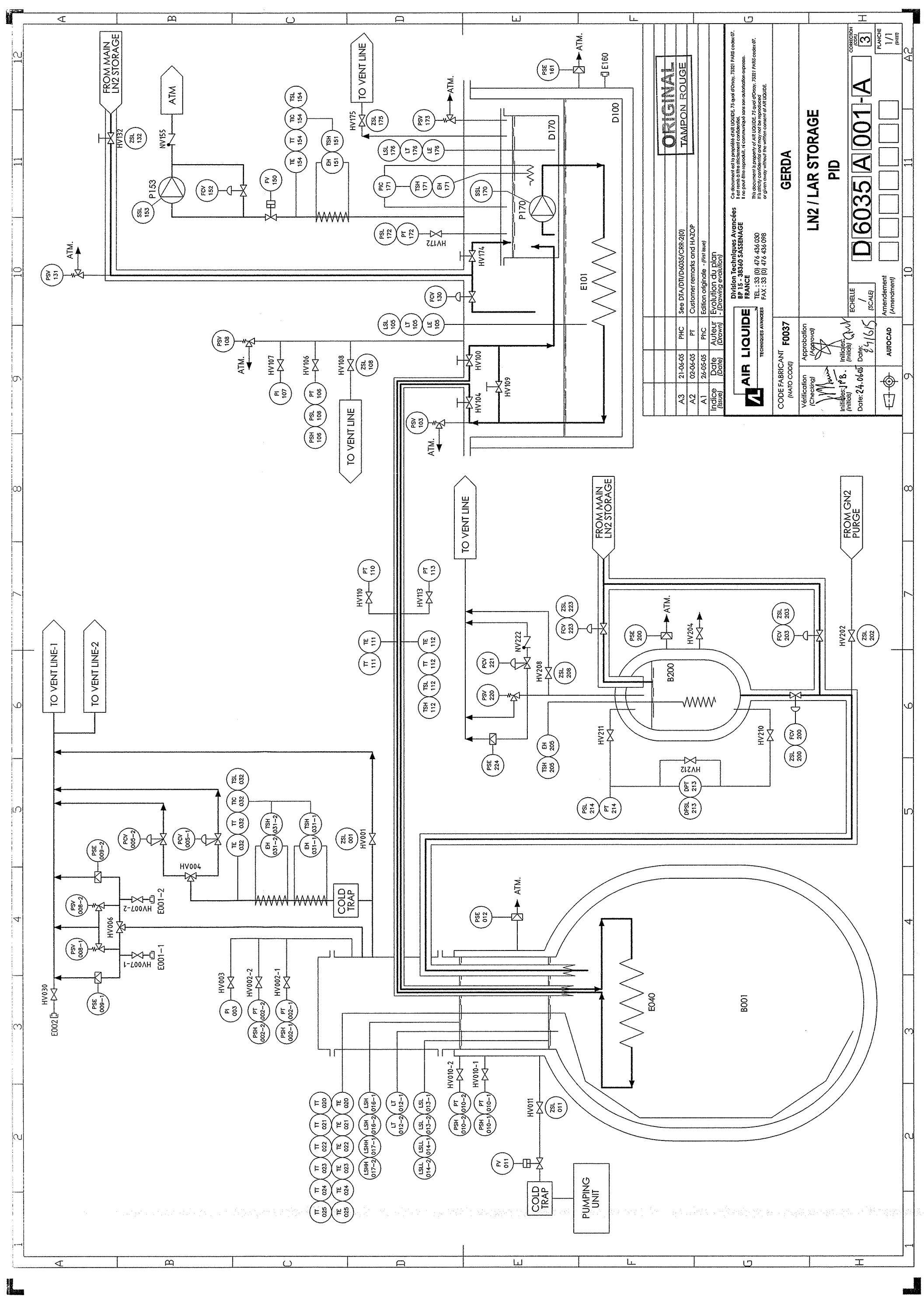

Figure 6: Piping and Instrumentation Diagram (PID) for the cryogenic infrastructure.

7 Water tank

The definitve engineering project of the water tank (WT), together with the constrution plan, has been completed in July 2005. It will be made in stainless steel (316AL or equivalent). Fig. 7 shows a side view of the water tank, the cryostat, the superstructure, and the lock inside the penthouse as conceived before the third wall recommendation. In parallel the design of the laboratory building and of the superstructure - wich are under the responsibility of the Laboratory - was developed. The purpose is to select a single company responsible for the whole complex. In May 2005 INFN funded the water tank on the 2005 and 2006 budgets. As a consequence, from the administative point of view, the tender can start. Tendering is a long procedure with an estimated duration of 6 months. Tendering will be under the 'integrated' form, meaning that the winner will be reponsible of the executive project too (which is dependent on the company's technology). In order to decouple as much as possible the construction of the WT from the completion and insertion of the cryostat, the construction plan foresees to leave initially a part, approximatly 4.5 m x 6 m height, open for the insertion of the cryostat. After insertion, the construction of the tank will be completed by final welding. The ongoing works on the hall floor by the Commisoner include the insertion of the fixing pins of the cryostat; their positions have been defined. The safety issues related principally to the possible spills of LN2 in water have been carefully considered by the LNGS and GERDA. Following the recommendation of the LNGS safety experts, the GERDA collaboration is presently studying the implementation of an additional wall as detailed in the previous section. Two materials are being considered for this third wall: OFE copper and LEXAN. Even if it already appears that the final choice should not interfere with either the Water Tank nor the cryostat, we decided to stand by the WT tendering till October.

8 Infrastructure on top of vessel

The penthouse design was adjusted to several infrastructural requests, resulting in the design depicted in Fig. 7.

The clean-room design including service areas was modified accordingly. The lock-system design was adjusted to the specifications concerning pressures in the cryostat and the cabling needs. Cable tubes attached to the inner lock allow for modular cable exchanges.

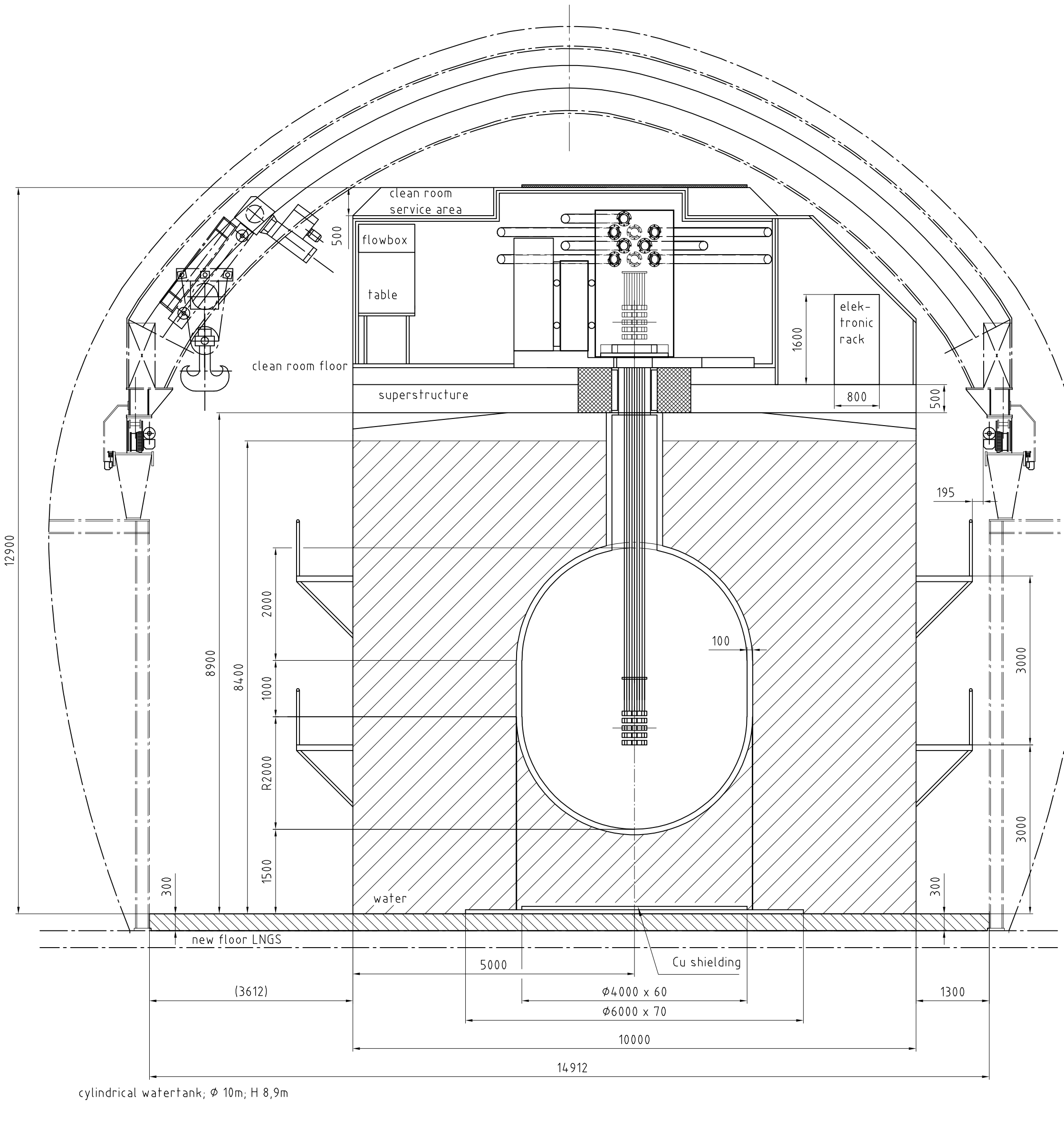

Figure 7: Vertical cut through the center of the experiment looking from the street. The recommended third wall between water and cryostat is not yet shown.

9 Muon veto system

For background reduction an active veto system will be installed at GERDA. Background produced by muons and their secondaries will be recognized by this system and consequently removed in the analysis. The layout of this system is being optimized by detailed Monte Carlo simulations (see section 10). Thereby, particular attention is focused on those events, where energy is deposited simultaneously in the Ge array, or more specific when the energy deposition amounts to about $Q_{\beta\beta} = 2$ MeV.

The veto will consist of two main parts: (i) a set of 3 cm thick plastic scintillators covering an active area of about 25 m^2 on top of the penthouse, and (ii) a water Cherenkov detector which uses the water shield as medium and about 80 photomultipliers for detecting the emitted light. For yielding good performance, the detection of the light emitted below the cryostat is found to be crucial.

Photomultipliers of type ET9350KB will be used and have been already ordered. Each photomultiplier will be operated in a water-tight encapsulation which has proven its reliability in the BOREXINO experiment. Photomultiplier and electronics are connected by cables, again of BOREXINO design, which penetrate through the water tank's roof through six DN250 flanges. To keep the number of photomultipliers reasonably low, both the additonal wall as well as the (outer) wall of the water tank will be covered with VM2000 reflector foil. The influence of the water pH value as well as the possibility of using a wavelength shifter in the water and in the PET windows of the photomultiplier encapsulation are under study.

A plan for the installation of the photomultipliers is being developped including the specifications of the necessary scaffolding equipment.

10 Simulations and background studies

The two main simulation efforts over the past months were: (1) evaluation of the cosmic-ray-induced background and optimization of the Cherenkov muon veto; (2) evaluation of the background due to radioactive contaminations in the crystals and in the supporting structures. The simulations have been carried out using the Geant4-based MaGe framework, which is developed and updated jointly with the Majorana collaboration.

10.1 Muons and muon veto

The contribution of cosmic-ray muons (and of the induced neutrons in the Gerda experimental set-up) to the background index at $Q_{\beta\beta}$ is summarized in Tab. 2 for Phase I. The anticoincidence cut between the 9 crystals of Phase I can reduce the background of a factor of 4.5, down to $4.1 \cdot 10^{-4}$ counts/keV kg y, which meets the goal, 10^{-2} counts/keV kg y. On the other hand, in order to gain an extra "safety margin", even in the perspective of the Phase II, the instrumentation of the water tank as a Cherenkov detector appears highly preferable already in Phase I. The background index with the Cherenkov muon veto is lower than $3 \cdot 10^{-5}$ counts/keV kg y (at 95% CL) for 120-MeV energy threshold, which can be achieved with about 80 PMTs.

Condition	Background index (counts/keV kg y) Phase I
No cuts	$(1.9 \pm 0.1) \cdot 10^{-3}$
Crystal anticoincidence	$(4.1 \pm 0.5) \cdot 10^{-4}$
Anticoincidence and plastic μ veto	$(3.5 \pm 0.6) \cdot 10^{-4}$
Anticoincidence and Cherenkov μ veto	$< 3 \cdot 10^{-5}$ at 95% CL
Anticoincidence and both μ vetoes	$< 3 \cdot 10^{-5}$ at 95% CL

Table 2: Background index in the range 1.5 → 2.5 MeV for different veto scenarios. The threshold for Ge detectors is 50 keV. The quoted errors are the statistical ones.

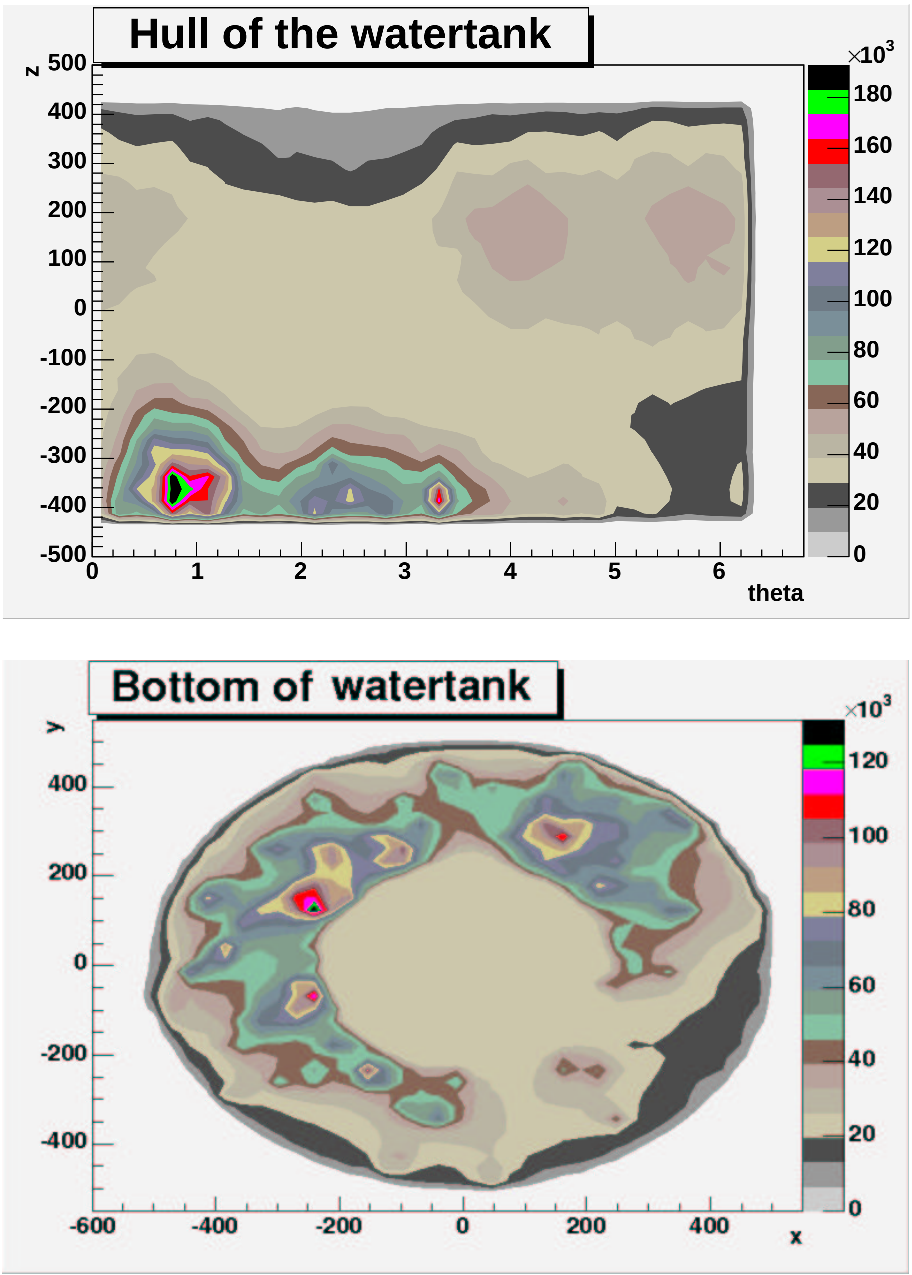

Figure 8: Cherenkov photon intensity maps for bottom and unfolded hull of the watertank of muon events which have an energy deposition in the germanium crystals in the range of 1.5 MeV to 3.0 MeV. The photons centrally under the cryostat will be detected in the 'lower pillbox' and are not shown here. The assymmetry of the photon distribution reflects the particular angular distribution of the underground muon flux.

In a first Monte Carlo simulation, muons are selected which deposit energy in the Germanium detectors. Until now, about 140 million muons have been simulated, using the Gran Sasso muon distribution. About 20000 muons of those caused energy deposition in the crystals. Out of those 260 muons were identified as 'dangerous', ie. the energy deposition in one or more germanium crystals was in the range of 1.5 MeV to 3.0 MeV.
For those muons, specific Monte Carlo simulations have been run to reconstruct the photon maps in the water tank and to optimize the placement of the PMTs. For instance, Fig. 8 shows the photon map of the hull and bottom of the water tank.

Configurations with 72 and 78 PMTs are being explored: two seperated boxes above ("upper pillbox") and below ("lower pillbox") the cryostat contain each a set of four PMTs, this is the "inner veto" and the rest are attached to the watertank walls, this is the "outer veto". VM2000 is used as a light reflector and wavelengthshifter.

Details of the veto trigger have still to be defined, but the results of the MC already show that an efficiency of more than 98 % for the dangerous muons can easily be achieved. The Monte Carlo simulations also show the importance of the combination of inner and outer veto because the outer veto alone would only detect about half and the inner veto about 80 % of the dangerous muons.

10.2 Radioactive contamination

Detailed Monte Carlo simulations have been performed for possible contaminations of the crystals, the cabling and the support structure. The geometry used in the calculations is that of Phase II. As a measure of the background suppression the survival probability is defined as the fraction of generated background events that "survive" the signal selection, i.e. an anti-coincidence requirement between segments and energy deposition within ± 5 keV around the $Q_{\beta\beta}$ value. The survival probabilities for several isotopes (^{226}Ra, ^{228}Th, ^{60}Co and ^{68}Ge) were obtained for each detector component and are summarized in Table 3. Where needed, a high-statistics calculation has been performed. In particular, this has been done for the strong gamma lines of ^{208}Tl and ^{214}Bi.

Material	Mass [g/det]	Contamination	SP [10^{-6}]
Crystal			
Germanium	2400	Ra-226	780
		Th-228	170
		Co-60	65
		Ge-68	180
Surface	-	Pb-210	160
		Th-228	1030
Holder			
Copper	31	Ra-226	50
		Th-228	110
		Co-60	≤ 31
Teflon	7	Ra-226	50
		Th-228	70
Cables			
Copper	1.3	Ra-226	1630
		Th-228	1110
		Co-60	80
Kapton	0.8	Ra-226	260
		Th-228	250
		Co-60	10
Bond pads and wires			
Copper	0.04	Ra-226	150
		Th-228	60
		Co-60	40
Nickel	0.04	Ra-226	160
		Th-228	130
		Co-60	≤ 31
Gold	$5.6 \cdot 10^{-4}$	Ra-226	200
		Th-228	40
		Co-60	≤ 31
Aluminum	$8.2 \cdot 10^{-5}$	Ra-226	410
		Th-228	170
		Co-60	≤ 31
Support Strings			
Copper	20	Ra-226	0
		Th-228	0
		Co-60	10
Electronics			
Misc.	(3/4) 100	Ra-226	8
		Th-228	46
		Co-60	≤ 31

Table 3: Summary of background contributions with an anti-coincidence requirement between segments. SP (=survival probability) is the fraction of generated background events that survive the anti-coincidence cut and deposit energy within ± 5 keV from $Q_{\beta\beta}$.

11 Material screening

In the reporting period the material screening by gamma spectrometry has been continued. Moreover, complementary ICP-MS measurements were performed for almost all samples which were assayed by gamma spectrometry. Another important activity concerns the purity control of argon in terms of ^{222}Rn and the development of purification procedures. Also surface impurity studies have been continued.

11.1 Gamma spectrometry and ICP-MS

In the first design of GERDA the copper for the cryostat was supposed to contain a small amount of phosphorus (DHP copper). Recently it was decided to use oxygen-free (OFE) copper for the cryostat which does not require additional phosphorus. The series of measurements performed for the DHP copper was useful to start a comparison of the low-level counting capabilities of different groups in GERDA. The comparison will be continued and will eventually help to optimize the distribution of future samples among the institutes. A screening measurement of OFE copper with the GeMPI detector at Gran Sasso has been performed. The results will be available soon.

Often the mass of available samples is too small to get sufficiently low detection limits with gamma spectrometry. Screening techniques which measure directly the long-lived progenitor nuclides of the natural decay chains such as ICP-MS and NAA require only a very small amount of material. However, the results are only meaningful for GERDA if the secular equilibrium in the chains is not broken. This has been studied by comparing ICP-MS results with those from gamma spectrometry for the same samples. Measurements on more than 10 samples have shown that the equilibrium in the uranium chain is often broken. Thus ICP-MS and NAA techniques alone will not be sufficient for material qualification and whenever possible, we will perform final quality checks using gamma spectrometry and the ^{222}Rn emanation technique.

11.2 Argon purity

Liquid argon is an alternative for liquid nitrogen in GERDA. The same stringent purity requirements as for nitrogen have to be fulfilled. We investigated the initial ^{222}Rn concentration in argon from the German Company Westfalen AG. For argon 5.0 we found a high activity of 8 mBq/m^3 (STP). For the better quality argon 6.0 the initial activity is significantly lower (0.4 mBq/m^3 (STP)). Due to the decay of ^{222}Rn these concentrations decrease with time and are finally given by the ^{222}Rn emanation rate of the specific storage tanks. We have measured the ^{222}Rn saturation activity of two standard cryogenic storage tanks after the cryo-liquid had evaporated. The results were 40 mBq and 190 mBq for a 600 liter tank and a 3500 liter tank, respectively. Under the assumtion of equally distributed radon in the argon the final ^{222}Rn concentration in the completely filled 3500 liter tank is 0.07 mBq/m^3 (STP). However, we have observed that radon predominantly sticks to cold walls, hence the ^{222}Rn concentration in the argon will even be lower.

For a further radon reduction we have checked the potential of argon purification by cryo-adsorption of radon on activated carbon. The purification of argon in the gas phase is highly efficient. The purified argon has a ^{222}Rn activity of less than 0.5 μBq/m^3 (STP). Also the purification in the liquid phase works well although it requires bigger carbon columns to obtain the same reduction factors. Given these results it is clear that from the radiopurity point of view both gases, nitrogen and argon, meet the specifications for GERDA.

References

[1] A. Pullia et al., IEEE Trans. Nucl. Scien. 49 (2002) 5.
[2] P.F. Manfredi et al., NIM A380 (1996) 308-311.
[3] www.amptek.com/a250.html